J. Mater. Eng. (1989) 11:149–157

Fiber Metal Acoustic Material for Gas Turbine Exhaust Environments

Michael S. Beaton

Abstract. FELTMETAL®[1] fiber metal acoustic materials function as broad band acoustic absorbers. Their acoustic energy absorbance occurs through viscous flow losses as sound waves pass through the tortuous pore structure of the material. Exhaust gas noise attenuation requirements are reviewed. Their selection process for higher performance materials is discused. A new FELTMETAL® fiber metal acoustic material has been designed for use in gas turbine auxiliary power unit exhaust environments without supplemental cooling. The physical and acoustic properties of mesh supported fiber metal acoustic medium FM 827 are discussed. Exposure testing was conducted under conditions which simulated auxiliary power unit operation. Weight gain and tensile strength data as a function of time of exposure at 650° C (1202° F) are reported. Fabrication of components with fiber metal acoustic materials is easily accomplished using standard roll forming and gas tungsten arc welding practices.

INTRODUCTION

FELTMETAL® fiber metal acoustic media (sintered stainless steel fiber structures in thin sheet form) are used to reduce the noise output from gas turbine engines, including the auxiliary power units (APUs) on commercial aircraft. Gas turbine exhaust silencers are exposed to the products of combustion of jet fuel. The severity of this environment will vary with the design parameters of each application, with ambient conditions, and with other factors. The temperature limit for the use of a given acoustic medium is primarily determined by the material (alloy) from which the medium is fabricated. New APU installation designs have imposed higher operating temperatures for acoustic media. Higher performance media capable of longer operating life at higher temperatures are required for these applications. This report describes a test program whose objective is to determine the suitability of a new acoustic attenuation material for operation in the 650° C temperature range.

[1]FELTMETAL is a registered trademark of the Brunswick Corporation.

The author is with Brunswick Corporation, Technetics Division, Energy Conservation Systems, 2000 Brunswick Lane, DeLand, FL 32724, USA.

NOISE REDUCTION

The gas turbine engine represents a source of noise of wide frequency range. The jet itself generates noise for several engine diameters downstream from the actual exit. The frequeny of the noise decreases with increasing distance from the engine exit point [1]. In addition to the jet, noise is created by the fan—both radiating forward from the fan and at the fan bypass exit. The compressor, turbine, and combustors also add their own frequency contributions to the total engine noise spectrum. Efforts to curb the noise generated by gas turbine engines have been exerted since the introduction of jets for commercial aircraft [2].

Acoustic attenuation media may be point reactive or bulk absorbing in nature [3]. Bulk absorbing media may be physically unwieldy or mechanically unsuitable for use in aircraft engine applications. A typical duct silencer might consist of a thin sheet of porous material with a flat, smooth surface backed by cavities of depth appropriate to the frequency of sound being generated. This arrangement provides noise attenuation over a broad band of frequency with a lightweight structure. The smooth flow surface of the fiber metal sheet keeps self-noise generation low [4]. In the fiber metal structure, the pores are interconnected, with many tortuous flow paths. The energy of an acoustic wave tends to dissipate within a porous material through viscous flow losses as the wave passes through the

porous medium. Among the FELTMETAL® fiber metal acoustic materials, layers of screen mesh may be employed to structurally reinforce the material for application [5].

FIBER METAL ACOUSTIC MATERIALS

FELTMETAL® fiber metal acoustic materials are thin sheets of carefully controlled aggregates of metal fibers. The fibers are joined into a contiguous mass by sintering. A given product may incorporate more than one fiber size or type, or layers of screen may be used to structurally reinforce the material and assure product durability. Final product strength and acoustical properties are controlled by the sintering schedule and by compressing the sheet to a predetermined density. The density and fiber diameter control the pore size and determine the specific surface area. These factors have controlling influences on the air flow resistance of the acoustic material.

Most of the FELTMETAL® fiber metal acoustic attenuation materials are fabricated from Type 347 stainless steel. However, any alloy which can be drawn into wire and sintered can be used to produce these materials. The Type 347 materials function well in applications with temperatures up to 540° C (1004° F). FM 134 is a widely used acoustic material with 35 rayl (cgs) flow resistance. Physical properties of this material are listed in Table 1. This material is typically used in exhaust silencers for gas turbine auxiliary power units for commercial aircraft.

A new APU silencer design required a silencing medium of the same acoustical performance as FM 134, yet capable of operating continuously at 650° C (1202° F). The gas turbine exhaust gases are products of combustion of jet fuel, which are typically oxygen rich and contain sulfur. Therefore, the design of a material for the new application required consideration of both the temperature and the chemical nature of the environment.

The combustion of fossil fuels presents materials problems mainly due to impurities. Many studies of high temperature corrosion of engine and power plant components have been carried out [6,7,8,9,10,11,12]. Impurities deposit on operating hardware and can lead to corrosive reaction at the elevated temperatures of operation. Sulfidation is the most studied class of reactions relating to fossil energy conversion applications [13]. While the corrosion mechanisms vary depending upon the level of sulfur concentration and the oxidation potential of the system, it is generally recognized that greater resistance to the corrosive reactions will be realized as chromium content is increased, and that additions of secondary oxide forming elements, including aluminum, to high chromium alloys tend to strongly enhance the resistane to hot corrosion.

Table 1. Properties of Selected Fiber Metal Products

Alloy	Composition	CTE × 10^6, 1/°F (1/°C)	Fiber Diam, μm	FM desig.
Type 347	Fe–18Cr–11Ni	10.4 (19.0)	102	FM 134
Type 430	Fe–16Cr	6.6 (11.9)	25–85	FM 1304
Hoskins 875	Fe–22Cr–5.5Al	6.3 (11.3)	142	FM 1401

In selecting an alloy for the new material, consideration was given to corrosion resistance, fabricability, durability in service, cost, and availability. The austenitic stainless steels, which include Type 347, have good corrosion and oxidation resistance at lower temperatures. However, the alloys in this group have high coefficients of thermal expansion (CTEs). Ferritic stainless steels generally have lower CTEs than austenitics, and also lower ultimate tensile strengths [14]. For screening tests, fiber metal materials of three different alloys were selected. Table 1 lists those materials selected along with several important properties.

The Type 347 fiber metal FM 134 was chosen as the control material for the test series. Its extensive field performance is available for comparison against actual operating conditions. The Type 430 fiber metal was selected as a nominal ferritic stainless steel. The configuration of this fiber metal is not optimized for acoustic attenuation service, but the physical properties would allow direct comparison in environmental exposure tests. The Hoskins 875 fiber metal is a material configured for high temperature oxidation resistance. Its composition includes substantial aluminum, which renders the alloy highly resistant to oxidation, and to sulfidation in a highly oxidizing environment.

Ratings of operating temperature and time for FM 1401 were established through thermal oxidation exposure testing in still air [15]. Weight gain data collected for temperatures of 1900, 2000, and 2100° F (1038, 1093, and 1149° C) are shown in Figure 1. At 1900° F (1038° C), stable oxidation behavior was observed throughout the 3115 hr testing duration. At 2000° F (1093° C) and 2100° F (1149° C), stable oxidation continued up to 3.5–4.0% weight gain. Above 4% weight gain oxidation behavior changed. Product life is determined by the accelerated oxidation behavior. For 1900° F (1038° C) exposure, the product life is estimated by extrapolation of the data to 4% weight gain. Product life ratings for FM 1401 at various temperatures are summarized in Figure 2.

SCREENING TESTS

The first round of testing consisted of material characterization (ultimate tensile testing and sample

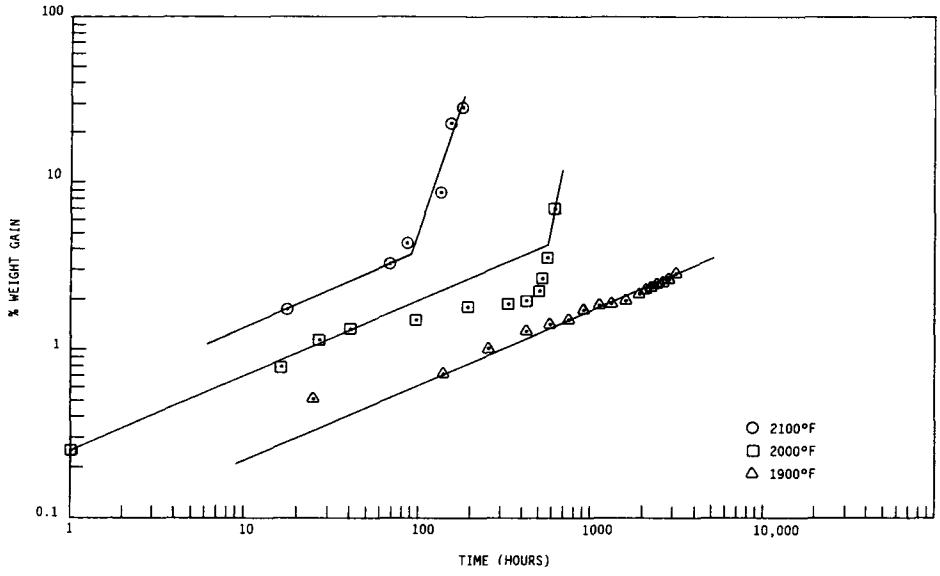

Fig. 1. Oxidation weight gain vs. time for Brunsbond® pad FM 1401 at three temperatures.

weighing) and oxidation in air. The target application temperature of 650° C (1202° F) was chosen for exposure of the specimens. The specimen base weights were recorded after a preoxidation treatment at 650° C for 0.1 hr, then weights were determined periodically thereafter. Figure 3 displays the weight gain as a function of time. Each data point is the average for three specimens. Each weight measurement imposed one thermal cycle to room temperature. After 1,000 hr of exposure and final weight measurement, the tensile strength of each specimen was determined. Table 2 lists the tensile strength and oxidation weight gain properties affected by the oxidation exposure.

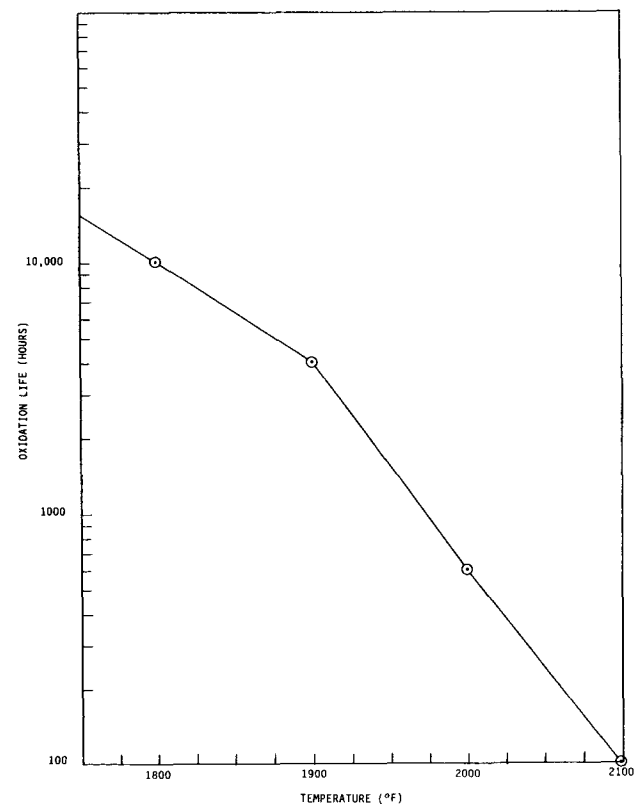

Fig. 2. Product life ratings for Brunsbond® pad FM 1401 at various temperatures.

Figure 3 shows that the T347 and the T430 fiber metals oxidized at similar rates for about the first day of exposure. However, at about three days of exposure, the rate of oxidation for the T347 fiber metal had increased to almost 10 times that of the T430 fiber metal. After the first "breakaway" in the T347 curve, the slope of the oxidation curve for that material leveled out to the same slope as in the initial stage of oxidation. By contrast, the T430 material oxidized at a constant rate throughout the entire 1000 hr period. The slope of the H875 curve is also constant, but yet one decade lower than that of the T430. Early data points for this curve are not included as they lie essentially on the abcissa.

The distinction in oxidation behavior between the austenitic product and ferritic products is related to the coefficients of thermal expansion of the alloys, which are listed in Table 1. The oxide scale which forms on the alloys has a lower CTE than the substrate alloys. The CTE for T430 is 36% lower than that for T347. The thermal stress generated in cooling the oxidized fibers is lower for the T430 than for the T347. This thermal stress is sufficient in the T347 material to cause spallation of the protective oxide layer and accelerated oxidation of the underlying fiber. Accelerated oxidation is represented by the "breakaway" section of the oxidation curve for the T347 material. In case of the T430 material , the thermal stress generated on cooling is below the spallation level and oxidation proceeds without the breakaway behavior.

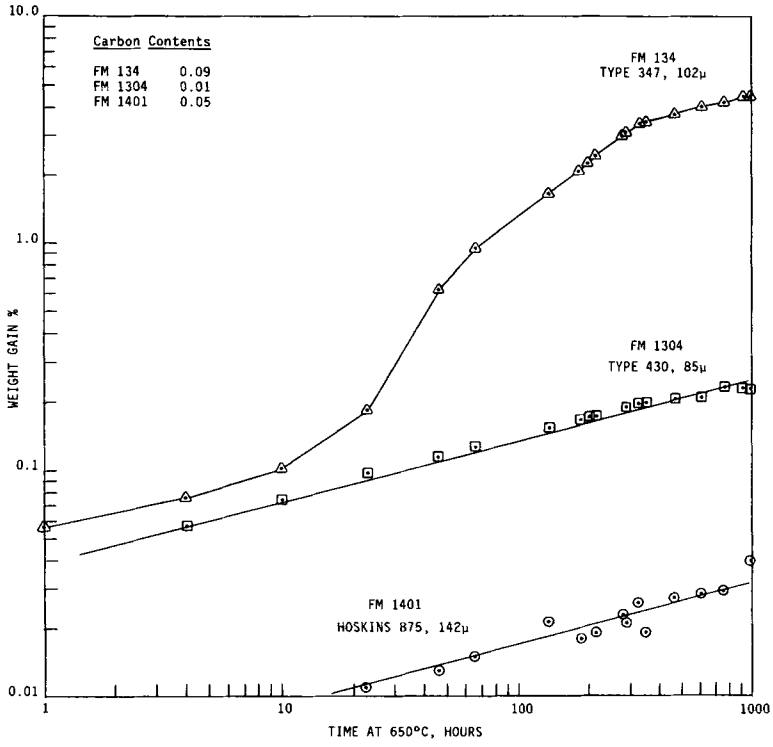

Fig. 3. Oxidation weight gain vs. time at 650° C for three fiber metal materials.

This phenomenon is treated in greater detail in [16]. The CTE for H875 is slightly less than for T430, so the thermal stress generated on cooling would be even less. This alloy's higher chromium and considerable aluminum contents promote the formation of aluminum oxide, or a mixed chromium–aluminum oxide, which greatly retards oxidation in the temperature range of the test.

The data in Table 2 show that the T347 material gained 4.32% of its original weight through the 1000 hr of oxidation exposure, and incurred a loss of tensile strength of 13.3%. In comparison, weight gain for the T430 material was only 0.22%, and the oxidized specimens had an average strength greater than the unoxidized control specimens. This apparent anomaly may be due to statistical differences of sampling pattern and material variation. The H875 material gained only 0.04% of original weight in the 1000 hr, with an apparent 6.3% strength decrease. A strength variation of ±10% is expected among the fiber metal specimens.

Table 2. Product Properties Affected by Oxidation

Product Number	Tensile Strength (Pretest) (MPa)	Tensile Strength (Post-test), (MPa)	Strength Change from Pretest, %	Oxidation Weight Gain, %
FM 134	15,345 (105.8)	13,306 (91.7)	−13.3	4.32
FM 1304	4,893 (33.7)	4,985 (34.4)	+1.9	0.22
FM 1401	4,997 (34.4)	4,680 (32.3)	−6.3	0.04

FLAME EXPOSURE TESTING

The screening test results confirmed the initial expectation that the ferritic stainless steels would withstand the rigors of oxidation exposure in the 650° F (1202° F) temperature range better than would the austenitic stainless steel. Based on this indication, a new material was specified. The material would be manufactured to the same acoustical properties as is FM 134 using the same fiber type and size with the exception that the alloy would be Hoskins 875. The new acoustic material was assigned the designation FM 827.

A test plan was formulated to expose both FM 134 and FM 827 to a simulated gas turbine exhaust environment. The conditions of exposure were selected to represent the operating conditions of an APU. An atmospheric pressure fuel atomizing combustor would burn Jet A fuel with excess air. Combustion could be carried out with fuel/air ratio up to 1:57, which corresponds to approximately 400% theoretical air for combustion. Sulfur level in the fuel was determined to be 0.033% by weight.

The specimen test configuration consisted of two

half cylinders—one of FM 827 and one of FM 134—mechanically held in a fixture. During exposure, the fixture was positioned within a shroud designed to contain the exhaust and assure uninterrupted immersion of the specimens in the exhaust. Throughout the test the specimen assembly was rotated through the flame. The specimen temperature was controlled by optical pyrometry to the desired set point. Fuel flow to the combustor was controlled based on the signal output from the optical pyrometer.

The exposure schedule consisted of 500 cycles. One cycle consists of 1 hr heating at 650° C followed by 15 min of cooling, without regard to heating or cooling rates. During the first and last heating cycle of each group of 100 cycles, the temperature was raised to 900° C (1652° F) for 1 min. At the end of each 100 cycles, the specimens were removed from the fixture and weighed to determine weight gain. After the dry weighing , the specimens were immersed in deionized water and reweighed. The water addition simulates rain and humidity exposure encountered in service. After 300 cycle hours were accumulated, specimens were removed for the determination of oxide layer thickness.

Figure 4 shows the specimen holding fixture with a cylindrical specimen in place. With the top plate removed, the specimens can be removed for weighing. Figure 5 is photo of the test rig during the shakedown run. The shroud is rotated in this photo to show the specimen fixture.

To accommodate the intermediate oxide layer thickness determination, the test procedure calls for four specimens: two larger specimens each comprise slightly less than half of a cylinder, while two smaller

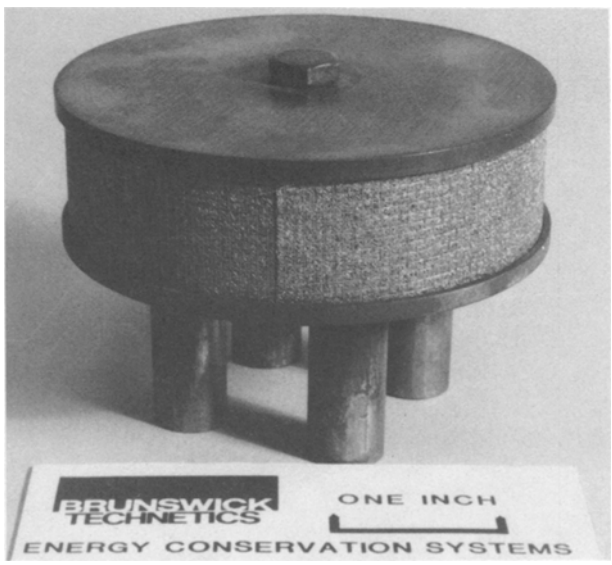

Fig. 4. Test apparatus: specimen holding fixture shown with cylindrical specimen.

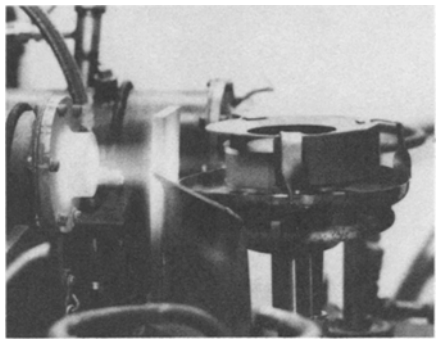

Fig. 5. Flame exposure test in progress.

specimens are included for removal after 300 cycles. Sectioning of the larger specimens is thus precluded and the progressive accumulation of weight gain data is not disturbed. The intermediate specimen was replaced by a duplicate so that temperature measurement was not affected. Prior to the test, ultimate tensile strengths of both materials were determined, and air flow resistances on the actual test specimens were measured for post-test comparison.

FLAME EXPOSURE TEST RESULTS

The specimens after 500 cycles are shown in Figure 6. The FM 827 specimens exhibit no dimensional distortion. However, the FM 134 specimens have sustained a permanent barreling about the specimen midline. Table 3 contains the specimen properties data as a function of time. Weight gain is plotted in Figure 7. As was observed in the screening test, the curve for the Fe–Cr–Al alloy FM 827 fiber metal is approximately one decade lower than that for the T347 FM 134. The total weight gains after 500 cycles are 1.38% and 13.05%, respectively. The tensile strength comparisons are even more dramatic. FM 827 retained 83% of its original tensile strength through the

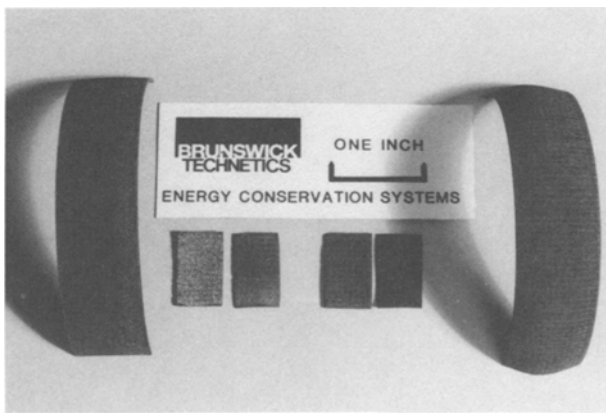

Fig. 6. Specimens after flame exposure.

Table 3. Specimen Properties as a Function of Time

Time, hr	0	100	200	300	400	500
			FM 134			
Wt. gain, %	0	4.5154	10.2647	11.2283	12.2246	13.0547
UTS, psi	18,121	—	—	—	—	4,060
(MPa)	(124.9)	—	—	—	—	(28.0)
Oxide thickness, μm	0	—	12.9[a]	—	—	37.3[a]
Airflow resistance, in. H_2O	0.65	—	—	—	—	[b]
	0.66	—	—	—	—	—
	0.83	—	—	—	—	2.25
	0.86	—	—	—	—	—
	0.69	—	—	—	—	—
	0.738					2.25
			FM 827			
Wt. gain, %	0	0.3462	0.7611	0.9348	1.1346	1.3792
UTS, psi	12,903		—	—	—	10,746
(MPa)	(89.0)	—				(74.1)
Oxide thickness, μm	0	—	[c]	—	—	[c]
Airflow resistance, in H_2O	0.77	—	—	—	—	1.02
	0.66	—	—	—	—	0.82
	0.7	—	—	—	—	0.81
	0.65	—	—	—	—	0.74
	0.67	—	—	—	—	0.94
	0.69					0.866

[a]Average of eight readings.
[b]Specimen fractured in measurement.
[c]Oxide layer thickness unresolved (400×) for 500 hr exposure. Flame deposition ("soot") on facing side of individual fibers over 24 μm thick.

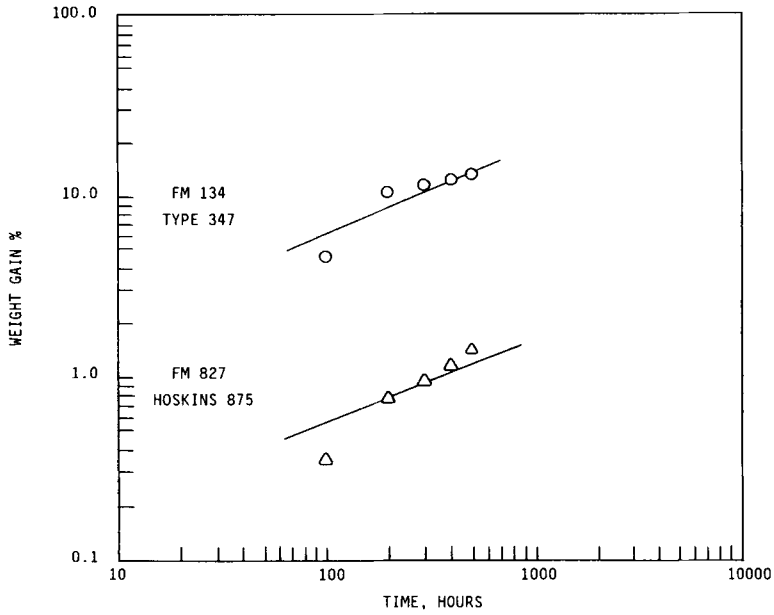

Fig. 7. Weight gain vs. time at 650° C in flame exposure for two fiber metal materials.

500 cycles of testing. In contrast, the FM 134 retained only 23% of its original tensile strength.

Air flow resistance readings were taken in five locations on the test specimens before exposure. The pressure drop readings for FM 827 increased by an average of 20.7%. Only one reading was obtained on the FM 134 specimen due to its distortion; the measured pressure drop in that location increased by 270%. Attempt to measure air flow in a second location resulted in fracture of the specimen and no further readings could be obtained.

Oxide layer thickness meaurements were made from metallographically prepared sections of the exposed specimens. The values listed in Table 2 are the average of eight readings of each cross section. Figure 8 exhibits the microstructure of the T347 fiber metal FM 134 after 500 hr of exposure. The entire material thickness is shown in the lower magnification view, Figure 8A. The light central areas are unoxidized metal; the gray surrounding material is the oxide formed on the fiber surfaces. The large amount of oxide accumulation has decreased the open area of the material, which is reflected in the air flow resistance measurements. The higher magnification view, Figure 8B, shows the oxide layer on an individual fiber in close detail. Cracks, globular discontinuities, and laminar growth of the oxide are readily visible. Cracking of the oxide layer tends to reduce its protective nature by exposing the base metal to further oxidation. Cracking is promoted by the large difference in thermal expansion rates between the oxide layer and the base metal.

The microstructure of the Fe–Cr–Al fiber metal FM 827 after 500 hr exposure is exhibited in Figure 9. The lower magnification view, Figure 9A, displays the entire material thickness. After this exposure time the open area of the structure remains unobstructed by oxide buildup on the fibers. However, a buildup

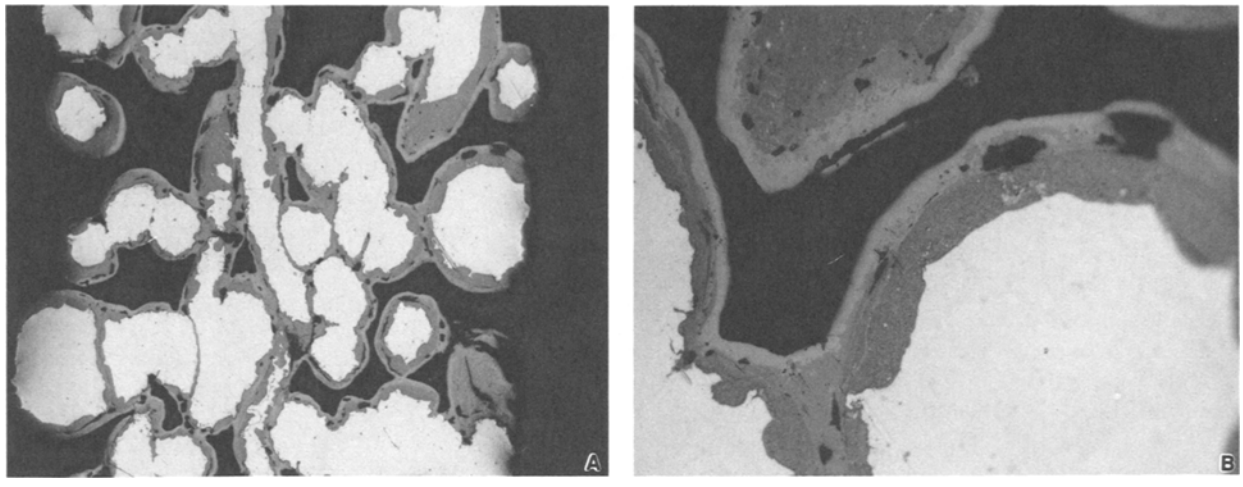

Fig. 8. Fiber metal FM 134 cross section after 500 hr flame exposure. (A) 200×, (B) 500×.

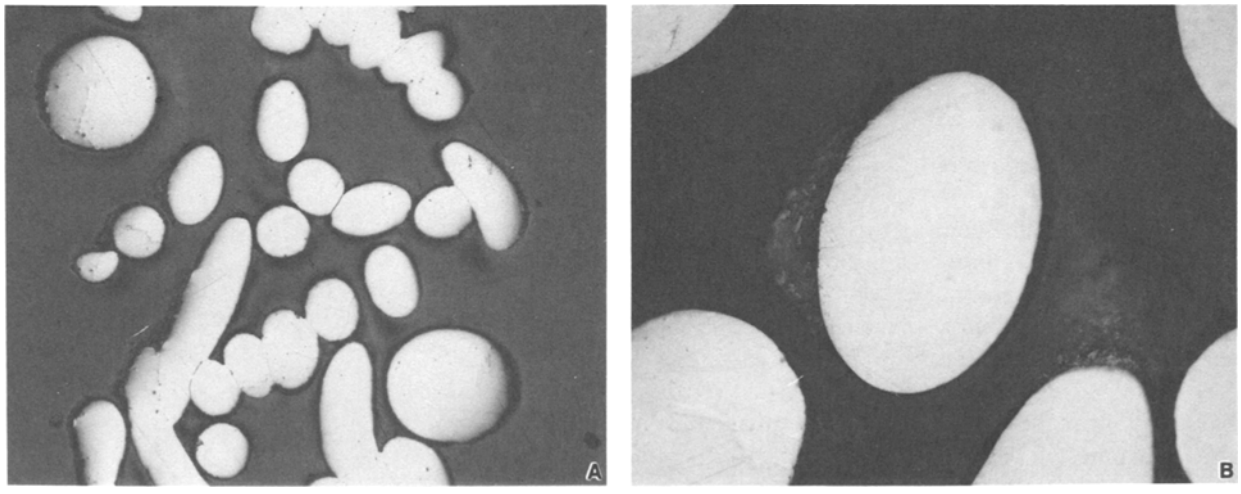

Fig. 9. Fiber metal FM 827 cross section after 500 hr flame exposure. (A) 200×, (B) 500×.

of material external to the fiber is observed on one side of the fibers in Figure 9A which have a line-of-sight passage to the outer boundary of the structure. As seen in Figure 9A, no buildup is present on the opposite side of the fiber. The buildup comprises material carried through the flame and deposited on the fibers and not an oxide generated from the fibers due to heating. Apart from the deposit, no other layer is measurable at the magnification of the photomicrograph.

The presence of an easily discernible deposit on the line-of-sight surfaces in the absence of a significant oxidation layer on other surfaces suggests that the weight gain data collected from the specimens in this test are biased high relative to the actual thermal oxidation response of the materials. As this effect was not anticipated in the test plan, no rigorous attempt was made to separate the contributions of the deposit and of base metal oxidation to the overall weight gain. Since the specimens were exposed to the same flame for the same length of time, the oxidation curves should be merely offset by some constant amount. The oxidation rate for the Fe–Cr–Al fiber metal FM 827 is no less than one tenth that of the austenitic stainless steel fiber metal.

FABRICABILITY

The utilization of the new acoustic fiber metal material requires that it be fabricated into a device for use in actual applications. The usual methods used to fabricate an exhaust silener include roll forming and welding. A typical exhaust silencer might be a cylinder approximately 230 mm (9 in.) in diameter and 914 mm (36 in.) long. In preparation of specimens for the flame test, cylinders of 76.2 mm (3 in.) diameter were roll formed with no damage to the material. Minimum forming limits will be less than 38.1 mm (1.5 in.) radius, although the actual limits have not been determined. The alloy itself has ductility limitations common to ferritic steels slow cooled from elevated temperatures. However, the ductility charateristics of the fiber metal structure itself are such that the alloy ductility only minimally affects the formability of the structure overall. The interwoven and interlocking fibers which comprise the fiber metal structure are individually required to bend or stretch only relatively small amounts during any given forming operation. Yet the sum of the shape changes of all the fibers involved facilitate operations such as roll forming.

Welding of the material is easily accomplished using the gas tungsten arc process. Because of the porous nature of the material, the use of filler metal is recommended. For FM 827 parts longer than approximately 100 mm (4 in.), the filler should be chosen such that thermal expansion coefficient is near that of the base alloy. Excellent weldability was obtained with the parent alloy Hoskins 875, and also with Type 430 stainless steel, Inconel 82, and nickel. For best results in the application for which FM 827 is designed, Hoskins 875 should be chosen. Type 430 or other ferritic stainless steels with at least 16% Cr (by weight) can also be used. Filler alloys with nickel should be avoided because of the sulfur content of the exhaust gases.

The technique applied to welding the fiber metal material is similar to that which might be used for sheet metal of the same composition. Weld specimens of an actual application length were produced using the following parameters:

- Joint preparation: sheared edge, butt joint without gap.
- Weld configuration: longitudinal seam, filler added.
- Work holding: chill fixturing on both sides of weld couple.
- Arc parameters:
- voltage—10 V DC straight polarity.
- current—21 A.
- gas—argon @ 15 cu ft/hr (7.1 L/min)(also backside shielding gas).
- high frequency superimposed to start arc.
- electrode—2% thoriated tungsten, 1.59 mm (1/16 in.) diameter, 22 deg tip angle, sharp point, 6.5 mm (0.256 in.) tip stickout, 3mm (0.125 in.) tip to work.

Specimens up to 991 mm (39 in.) long (maximum stock size) were welded for demonstration of capability. A silencer with FM 827 inner acoustic liner is shown in Figure 10.

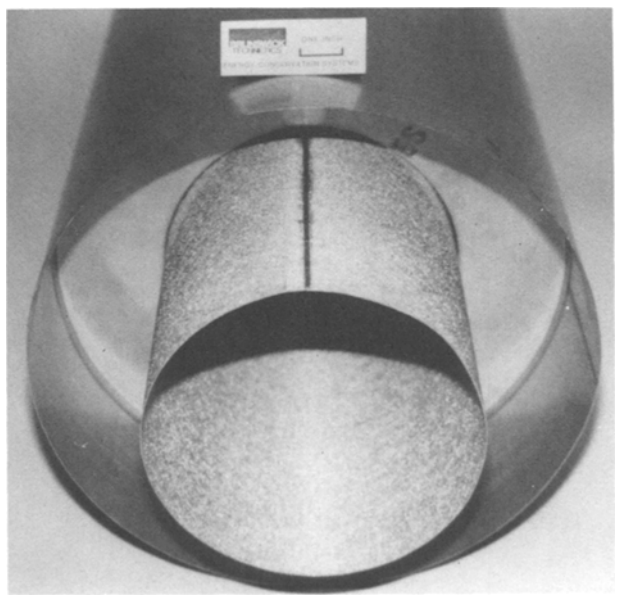

Fig. 10. Exhaust silencer with fiber metal FM 827 inner acoustic liner.

CONCLUSIONS

Fiber metal materials can be effectively utilized in noise reduction.

Fiber metal acoustic materials made from Type 347 stainless steel function well in applications with temperatures up to 540° C (1004° F).

FM 827, the new fiber metal acoustic material made from Hoskins 875, can operate continuously at 650° C (1202° F) in gas turbine exhaust conditions. A material of the same alloy and fiber type, larger fiber size and no mesh reinforcement is rated for 10,000 hr life at 982° C (1800° F).

FM 827 can be easily fabricable using standard roll forming and gas tungsten welding.

REFERENCES

1. P.A. Franken, "Jet Noise, " in *Noise Reduction*, L.L. Beranek, ed., McGraw-Hill, New York, 1960, p. 645ff.
2. J.D. Kester and A.A. Peracchio, "Noise Technology Requirements for Future Aircraft Powerplants," ASME paper 76-GT-69.
3. A.H. Nayfeh, J.E. Kaiser, and D.P. Telionis, "Acoustics of Aircraft Engine-Duct Systems," *AIAA Journal*, vol. 13, pp. 130–153, 1975.
4. A. Bauer, "Impedance Theory and Measurements of Single-and Multi-layer Liners in a Duct with Flow," AIAA paper no. 76-539, July, 1976.
5. J.I. Fisher and A.R. Erickson, "Properties of Fiber Metal Acoustically-Resistive Materials," presented at the Seventy-Second Meeting of The Acoustical Society of America, Nov. 3, 1966.
6. T. Zaizen, et al., "Oxidation and Hot-Corrosion Resistant High Aluminum Austenitic Stainless Steel," *J. Materials for Energy Systems*, vol. 2, no. 2, Sept. 1980, pp. 21–29.
7. F. Saegusa and D.A. Shores, "Corrosion Resistance of Superalloys in the Temperature Range 800–1300° F (430–700° C)," *J. Materials for Energy Systems*, vol. 4, no. 1, June, 1982, pp. 16–27.
8. R.W. Bradshaw and R.E. Stoltz, "Alloy Selection for Sulfidation–Oxidation Resistance in Coal Gasification Environments," *J. Materials for Energy Systems*, vol. 2, no. 1, June 1980, pp. 3–11.
9. T.C. Tiearney, Jr. and K. Natesan, "Metallic Corrosion in Simulated Low-BTU Coal-Gasification Atmospheres," *J. Materials for Energy Systems*, vol. 1, no. 4, March 1980, pp. 13–29.
10. Z.A. Foroulis and F.S. Petit, eds., *Proc. Symp. on Properties of High Temperature Alloys*, The Electrochemical Society, Princeton, New Jersey, 1976.
11. C.M. Packer and R.A. Perkins, "The Performance of MCrAl Alloys in Complex Coal Conversion Atmospheres," abstracted in *Materials and Components in Fossil Energy Applications, a DOE Newsletter*, No. 28, June 1, 1980.
12. G. Sorell, "Parametric Studies of Erosion–Corrosion of Alloys in High-Temperature Sulfidizing Environments," *Materials and Components in Fossil Energy Applications, a DOE Newsletter*, No. 69, Aug. 1, 1987.
13. E.E. Hoffman, ed., *Materials and Components in Fossil Energy Applications, a DOE Newsletter*, Special Index Edition II, July 1, 1984.
14. R.B. Gunia et al., "Wrought Stainless Steels," *Metals Handbook, 9th Edition, Volume 3*, American Society for Metals, Metals Park, Ohio, 1980, pp. 3–40.
15. R.P. Tolokan, unpublished research, 1986.
16. G.C. Wood, *Corros. Sci.*, vol. 2, (1962), p. 173.